PUR-II (SRU), 76709-95-0; POX-I (block copolymer), 109013-89-0; POX-II (block copolymer), 109013-88-9; PTR-I (block copolymer), 109013-91-4; PTR-II (block copolymer), 109013-90-3; $OCNC_6H_5$, 103-71-9; 4,4′-$OCNC_6H_4CH_2C_6H_4NCO$, 101-68-8; $OCN(CH_2)_6NCO$, 822-06-0; BuNCO, 111-36-4; $OCNC_6H_{10}CH_2C_6H_{10}NCO$, 5124-30-1; $C_6H_{11}NCO$, 3173-53-3.

References and Notes

(1) Speranza, G. P.; Peppel, W. J. *J. Org. Chem.* **1958**, *23*, 1922.
(2) Gulbins, K.; Hamann, K. *Angew. Chem.* **1958**, *70*, 705.
(3) Sandler, S. R.; Berg, F.; Kitazawa, G. *J. Appl. Polym. Sci.* **1965**, *9*, 1994.
(4) Herweh, J. E.; Foglia, T. A.; Swern, D. *J. Org. Chem.* **1968**, *33*, 4029.
(5) Herweh, J. E.; Kauffman, J. *Tetrahedron Lett.* **1971**, *12*, 809.
(6) Sandler, S. R.; *J. Polym. Sci., Polym. Chem. Ed.* **1967**, *5*, 1481.
(7) DiLeone, R. R. *Polym. Prepr. (Am. Chem. Soc., Div. Polym. Chem.)* **1968**, *9*, 642.
(8) Brown, D.; Wienert, J. *Angew. Makromol. Chem.* **1979**, *78*, 1.
(9) Herweh, J. E.; Whitmore, W. Y. *J. Polym. Sci., Polym. Chem. Ed.* **1970**, *8*, 2759.
(10) Bald, G.; Kretzschmar, K.; Markert, H.; Wimmer, M. *Angew. Makromol. Chem.* **1975**, *44*, 151.
(11) Kitayama, M.; Iseda, Y.; Odaka, F.; Anzai, S.; Irako, K. *Rubber Chem. Technol.* **1980**, *53*, 1.
(12) Pankratov, V. A.; Frenkel, T. M.; Fainleib, A. M. *Rus. Chem. Rev. (Engl. Transl.)* **1983**, *52* (6), 576.
(13) Kordomenos, P. I.; Kresta, J. E. *Macromolecules* **1981**, *14*, 1434.
(14) Coleman, G. H.; Hadler, B. C.; Sapp, R. W. U.S. Patent 2 331 265, 1943.
(15) David, D. J.; Stanley, H. B. *High Polymers*; Wiley-Interscience: New York, 1969; Vol. XVI, Part III, p 115.
(16) Dijkstra, R.; Dahmen, A. M. F. *Anal. Chim. Acta* **1964**, *31*, 38.
(17) Korshak, V. V. *Vysokomol. Soedin., Ser. A* **1974**, 16, 926.
(18) Khalturinskii, N. A.; Berlin, A. A. *Rus. Chem. Rev. (Engl. Transl.)* **1983**, *52*, 1171.
(19) Korshak, V. V. *Khimicheskoe Stroenie I Temperaturnye Kharakteristiki Polimerov*; Izdatelstvo "Nauka": Moskva, 1970; p 272.
(20) Mathur, G.; Kresta, J. E.; Frisch, K. C. *Adv. Urethane Sci. Technol.* **1978**, *6*, 103; Technomics Publ.
(21) Paterson-Jones, J. C. *J. Appl. Polym. Sci.* **1975**, *19*, 391.
(22) Bowen, D. O. *Mod. Plast.* **1967**, *8*, 127.
(23) Paterson-Jones, J. C.; Percy, V. A.; Giles, R. G. F.; Stephen, A. M. *J. Appl. Polym. Sci.* **1973**, *17*, 1867.
(24) Paterson-Jones, J. C.; Percy, V. A.; Giles, R. G. F.; Stephen, A. M. *J. Appl. Polym. Sci.* **1973**, *17*, 1877.
(25) Leisegang, E. C.; Stephen, A. M.; Paterson-Jones, J. C. *J. Appl. Polym. Sci.* **1970**, *14*, 1961.
(26) Keenan, M. A.; Smith, D. A. *J. Appl. Polym. Sci.* **1967**, *11*, 1009.
(27) Freeman, I.; Frost, L.; Bower, G.; Taylor, E. *SPE Trans.* **1965**, *5* (2), 75.
(28) Danilina, L. I.; Muramtsev, V. I.; Prvednikov, A. N. *Polym. Sci. USSR, (Engl. Transl.)* **1975**, *17*, 2984.
(29) Winslow, F. H.; Matreyck, W. *J. Polym. Sci.* **1956**, *23*, 315.
(30) Bruck, S. D. *Polym. Prepr. (Am. Chem. Soc., Div. Polym. Chem.)* **1965**, *6*, 766.
(31) Bruck, S. D. *J. Polym. Sci., Part C* **1967**, *17*, 169.

Dipole Orientation in a Liquid-Crystal Polymer: A Study by Electric Field FTIR

Bruce M. Landreth and Samuel I. Stupp*

Department of Materials Science and Engineering, University of Illinois at Urbana—Champaign, Urbana, Illinois 61801. *Received December 1, 1986*

ABSTRACT: A dynamic study of dipole alignment in a main-chain liquid-crystal polymer exposed to an electric field revealed some fundamental properties of these macromolecules. The polymer studied was the polycondensate of 40 mol % poly(ethylene terephthalate) and 60 mol % *p*-acetoxybenzoic acid. Spectroscopic analysis of attenuated infrared reflections during application of an electric field allowed us to measure the spatial alignment of ester dipole moments. When poling occurs before or during the solid to liquid-crystal transformation, one observes a relatively fast dielectric alignment which remains stable in the liquid-crystal phase. When the liquid crystal is solidified under the field the extent of polar alignment for moments nearly orthogonal to the backbone could lie in the range of 4–10%. This range suggests that interchain dipolar coupling is an important phenomenon in these polymers. On this basis one may also expect that localized ferroelectric ordering enhances cooperative behavior during the transition from "poled" solid to liquid crystal. The observed phenomena could be useful in the formation of polymeric solids with electrical or nonlinear optical properties.

Introduction

Weak external fields can induce long-range molecular reorientation in liquid crystals.[1,2] The field-induced molecular alignment disappears for the most part after crystallization occurs at lower temperatures. However, when the molecules of the liquid crystal have polymeric dimensions it might be possible in some cases to freeze the alignment in the solid state. Long relaxation times and the absence or slow rate of three-dimensional crystallization are among the factors that may allow vitrification of the aligned state. The frozen orientational order could be significant since polymeric mesophases have high order parameters and are suspected to have lower symmetries than their small molecule analogues. Thus it might be possible to form microstructures with anisotropic properties after the vitrification or crystallization of polymer liquid crystal fluids aligned by electric, magnetic, flow, or surface fields. Our group reported previously on studies of backbone orientation by magnetic,[3] electric,[4] and surface fields[5] in main-chain liquid-crystal polymers. The present work focuses on field orientation on a finer scale, namely, the electric orientation of dipoles contained within the self-ordering rigid chains. The problem is of interest in the area of advanced polymers, given the special properties exhibited by poled solid phases. These include, among others, nonlinear optical properties and piezo- and pyroelectricity.

As predicted by the Langevin equation, low molecular weight polar fluids will experience only weak alignment even in strong electric fields. Field orientation of dipoles in a condensed phase which is both "polymeric" and "liquid crystalline" is a more complex and poorly understood phenomenon. In the high order parameter mesophases formed by polymers, it is not known if self-ordering characteristics would extend to a finer structural scale such as that of dipoles that are orthogonal or parallel to the backbone. It is this particular question that we have addressed in this paper. The measurements carried out

0024-9297/87/2220-2083$01.50/0

utilized FTIR in conjunction with a thermoelectric cell described in one of our earlier publications.[6] It is possible with this cell to measure spatial orientation of dipolar bonds during application of an electric field. This is accomplished through the use of an attenuated total reflection setup in which silicon crystals serve as both electrodes and optical paths for polarized infrared radiation. In this work we have modified the cell further to allow the possibility of a three-dimensional measurement of dipole orientation.

Experimental Section

Sample Preparation. The thermotropic liquid-crystal polymer used in this study was supplied in extruded pellet form courtesy of W. J. Jackson of Tennessee Eastman in Kingsport, TN. The polymer is the product of the high-temperature transesterification reaction of 60 mol % *p*-acetoxybenzoic acid (PHB) and 40 mol % poly(ethylene terephthalate) (PET). The synthesis of this and other PHB/PET copolymers is described in the literature,[7] and the products are reported to have normal molecular weight distributions with $15\,000 < \bar{M}_n < 20\,000$. Sample films 2 cm in diameter and approximately 240 μm thick were prepared by hot pressing extruded pellets, all of which were arranged such that the extrusion axis was perpendicular to the platens. This particular configuration of pellets was used to minimize uniaxial orientation in the plane of prepared films. Pressing was done in a specially designed mold[4] that applies a uniform thermal treatment over the 36 samples obtained in a given pressing. The platens of a Carver Model M press were heated to 230 °C prior to pressing and the mold was allowed to reach thermal equilibrium with the platens. The heat was then turned off and 50 000 lbs of force was applied to the mold assembly. Pressure was maintained while cooling to room temperature over a period of 7 h.

Spectroscopic Measurements. Spectroscopic measurements at elevated temperatures during application of electric fields required the construction of a thermoelectric cell. We reported earlier on the first version of this cell (standard cell).[6] In this standard cell, a 3 mm × 8 mm rectangular sample of material cut from the previously described pressed films was placed between two 10 mm × 5 mm × 1 mm silicon crystals. These crystals were single-pass parallelpipeds with 45° beveled edges which served as both electrodes and internal reflection elements. The thermoelectric cell and a Brewster angle polarizer mount onto a Harrick 4X variable-angle beam condenser placed in the sampling compartment of the FTIR spectrophotometer. For the present work a second thermoelectric cell was constructed which includes a provision for the rotation of the reflective crystal electrodes and sample through an angle of 90° (the rotating cell). A schematic drawing of the cell is shown in Figure 1. Square 10 mm × 10 mm × 1 mm reflection crystals with 45° beveled edges on all four sides are used in order to provide two optically equivalent single-pass parallelpiped reflection paths. This allows analysis of the sample in two different spatial orientations. The two halves of the cell are kept electrically insulated from one another by being mounted independently to the two separate parts of the base, which are in turn insulated from each other by an alumina ceramic spacer and nylon screws. The torque transmitting arm connecting the two sides of the cell consists of two brass fingers which do not quite meet and are coupled to one another by a ceramic tube. A thermocouple in direct contact with one silicon crystal is inserted through the long drive shaft and used for accurate temperature measurement during spectroscopic observation. The temperature of this cell was controlled with a Micristar programmable process controller from Research, Inc., Minneapolis, MN. The relative amount of heat supplied to each side was carefully balanced with a high-capacity variable resistor to ensure that no thermal gradient appeared across the cell. The heating elements in the cell are mounted vertically to minimize the amount of interference between the infrared radiation emitted from the ends of the heater tubes at high temperatures and the spectroscopic beam. The cell mounts onto the beam condenser and a special bracket was designed to hold the drive shaft in place during rotation.

In some experiments with the standard cell the thermal cycle involved heating as-pressed material from room temperature to 240 °C over a period of approximately 45 min. At 240 °C, the sample was in the nematic liquid-crystalline state. This temperature was maintained for a period of 1–3 h, followed in some cases by subsequent cooling back to room temperature. A pair of spectroscopic scans (one for each polarization) was taken at room temperature and at 25 °C intervals during the heating part of the cycle. Once 240 °C was reached, pairs of scans were taken continuously at first and then at regular intervals for the duration of the constant-temperature period. Scans were also taken at 25 °C intervals during the cooling portion of the cycle. The temperature was always held constant while the scans were being recorded. In some cases the electric field was applied during the constant-temperature period, and in others the field was applied at room temperature prior to heating. Thermal control experiments duplicated the above thermal cycle without the application of a field.

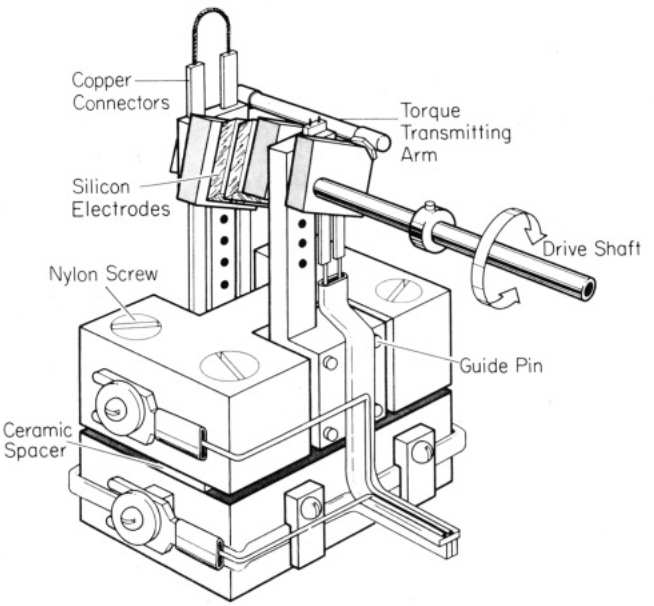

Figure 1. Schematic drawing of the rotating thermoelectric cell built for three-dimensional measurement of dipole orientation.

Experiments done in the rotating cell required a slightly different thermal cycle. Because of the rotation mechanism, very little force could be applied across the cell to clamp the crystals into place. It was therefore necessary to first melt samples in the cell in order to adhere them to the two reflection plates. For sample adhesion purposes the cell was heated from room temperature to 240 °C at 10 °C per min, holding at 240 °C for 10 min and then cooling to room temperature, again at 10 °C per minute. The actual spectroscopic measurements were then taken in a subsequent thermal cycle with heating and cooling rates controlled precisely to 5 °C per min and pausing for 3 min at 25 °C intervals to allow scans to be taken. During the constant-temperature period, a set of four scans was taken every 5 min. Analysis of the spectroscopic scans recorded as a function of time involved the digital integration of the C=O stretching band by using a frequency window from 1780 to 1656 cm^{-1}.

Results and Discussion

Flourney and Schaffers[8] showed that for the case where the real part of the index of refraction of the sample is isotropic, the resultant reflected intensities for the two polarizations are given by

$$-\ln R_{TE} = \alpha k_x \tag{1}$$

$$-\ln R_{TM} = \beta k_y + \gamma k_z \tag{2}$$

where k_x, k_y, and k_z are the absorption coefficients of the band along the three Cartesian directions defined in Figure 2. In the context of liquid crystals, the effect of any birefringence in the infrared region should be small and would only underestimate slightly the amount of molecular alignment inferred from reflectivity measurements. As shown in the Appendix, the constants α, β, and γ depend

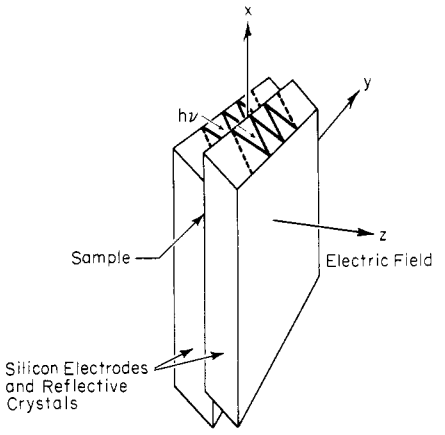

Figure 2. Schematic drawing of the two beveled-edge square silicon crystals which serve as electrodes and internal reflection elements. The coordinates shown indicate the electric field direction.

on the angle of incidence and the real parts of the refractive indices of both the reflection crystal and the sample material. We have used the values $\alpha = 1.16$, $\beta = 1.66$, and $\gamma = 2.16$ based on a refractive index of 1.65 for the experimental liquid-crystal polymer. This refractive index was estimated from previous dielectric constant measurements as a function of frequency for PHB homopolymer.[9] In this context, we point out that the constants α, β, and γ are relatively insensitive to changes in the value of n_2 within the range observed for polymers. From eq 1 and 2 it is straightforward to show that

$$A_{TE} = (N/2.303)\alpha k_x \tag{3}$$

$$A_{TM} = (N/2.303)(\beta k_y + \gamma k_z) \tag{4}$$

where N is the total number of reflections at both Si–sample interfaces (10 in the present case) and A_{TM} and A_{TE} are the respective integrated absorbances for the two polarizations of the infrared beam. It should be noted that the amplitude of the evanescent wave in the sample which is coupled with the TM-polarized propagating wave has a component along two of the Cartesian axes (y and z), while that which is coupled with the TE-polarized propagating wave has an amplitude along the x-axis only. Thus, although infrared intensity exists in all three spatial dimensions within the sample, it is still only possible to measure two independent absorbance values. This fact was the motivation for the construction of the rotating cell. Given an equivalent optical path for the infrared beam with the sample rotated through an angle of 90°, eq 3 and 4 become

$$A_{TE,90°} = (N/2.303)\alpha k_y \tag{5}$$

$$A_{TM,90°} = (N/2.303)(\beta k_x + \gamma k_z) \tag{6}$$

The combination of the two polarizations of incident radiation and the two possible orientations of the reflection crystals in the rotating cell yields four independent absorbance measurements to resolve the three coefficients k_x, k_y, and k_z. Using the experimentally measured values of k_x, k_y, and k_z, we calculated a fraction of dipoles aligned along the field direction, f_z, or a fraction of dipoles oriented in the plane of film samples, f_{xy}. These fractions were calculated by using the model that experimental absorbances result from a volume fraction of dipoles oriented randomly in three dimensions and from another fraction with uniaxial (f_z) or planar (f_{xy}) orientation.

In order to calculate f_z and f_{xy} we have used the models described by Fraser for interpretation of infrared dichroism. Let θ be the angle between the transition moment

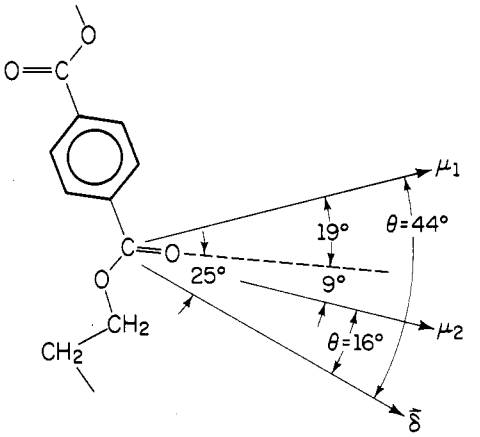

Figure 3. Repeating unit of poly(ethylene terephthalate) showing the angular relations between the ester dipole moment and the two possible directions of vibrational transition moments.

for the C=O stretching vibration and the ester group dipole moment and ϕ the average angle between dipole moments and the z-axis. One may then write the following expression:

$$\frac{k_z}{k_{x,y}} = \frac{2\cot^2\theta\cos^2\phi + \sin^2\phi}{\cot^2\theta\sin^2\phi(1 + \cos^2\phi)/2} \tag{7}$$

For the case where all dipoles are aligned parallel to the z-axis (the field direction),

$$\frac{k_z}{k_{x,y\ \text{axial}}} = 2\cot^2\theta = R_z \tag{8}$$

and for the case where all dipole moments are in the x–y plane, randomly distributed about the z-axis,

$$\frac{k_z}{k_{x,y\ \text{planar}}} = \frac{1}{\cot^2\theta + 1/2} = R_{x,y} \tag{9}$$

In order to interpret experimental measurements of $k_z/k_{x,y}$ in terms of dipolar orientation, we assume that a fraction of the dipoles is oriented along the field direction (f_z) and a fraction ($1 - f_z$) is randomly oriented in space. Similarly, we can assume a fraction $f_{x,y}$ is oriented in the plane of the film and a fraction ($1 - f_{x,y}$) is randomly oriented. We therefore write the following expressions,

$$f_z = \frac{(R - 1)(R_z + 2)}{(R_z - 1)(R + 2)} \qquad \text{for } R > 1 \tag{10}$$

or

$$f_{xy} = \frac{(R - 1)(R_{xy} + 2)}{(R_{xy} - 1)(R + 2)} \qquad \text{for } R < 1 \tag{11}$$

where R is the experimentally measured value of $k_z/k_{x,y}$. Note that in this model, $f_{xy} = f_z = 0$ when $R = 1$.

Figure 3 shows the repeating unit of PET. The strongest dipole moment is associated with the ester bond and makes an angle of approximately 25° with the C=O bond axis.[10] Studies on drawn PET concluded that the vibrational transition moment for the C=O stretching mode makes an angle of 76° with the molecular axis.[11,12] The bond itself makes an angle of 85° with the backbone axis[12] and therefore the transition moment makes either a 9° or a 19° angle with the bond axis. This corresponds to an angle θ of 16° or 44° between the vibrational transition moment and the dipole moment. Bradbury et al.[12] suggested 44° was the correct value based on a comparison with the amide group. Figure 4 shows plots of f_z and $f_{x,y}$ as a function of $k_z/k_{x,y}$ using values of θ = 16°, 44°, or 0°.

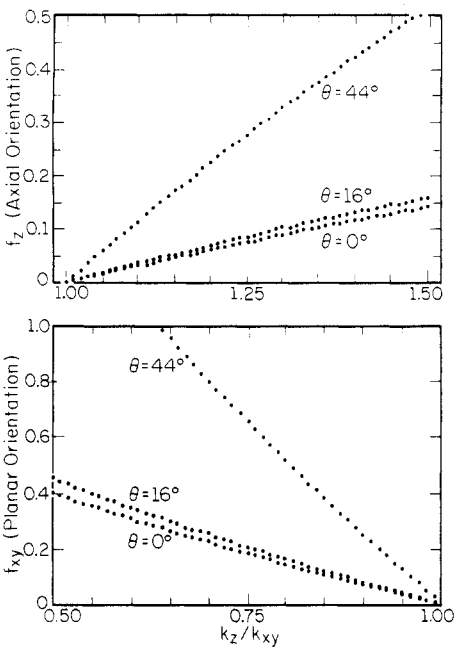

Figure 4. Plots showing the calculated fraction of ester dipoles oriented along the field direction (top) or the fraction contained within a plane normal to the field (bottom) as a function of the dichroic ratio k_z/k_{xy}. Each of the three curves shown in the graphs assumes a different angle between the vibrational transition moment and the dipole moment (44°, 16°, or 0°).

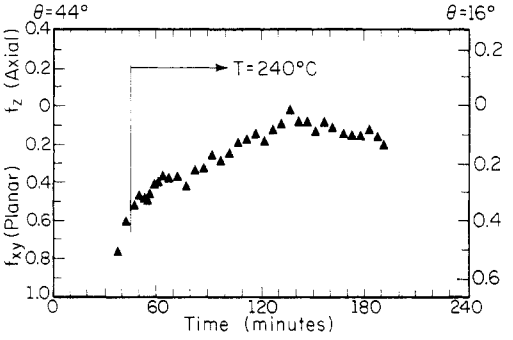

Figure 5. Fraction of oriented dipoles calculated with two different θ values as a function of time. The vertical line indicates the time at which the isothermal period begins.

Figure 5 shows a plot of the calculated fraction of ester dipoles contained in the x–y plane (f_{xy}) as a function of time in a thermal control sample. The data in Figure 5 were obtained by using the standard cell and therefore assuming that $k_x = k_y$. Values of the fraction on the right-hand ordinate were calculated by using a value of $\theta = 16°$ while those on the left were obtained with a value of $\theta = 44°$. The vertical line indicates the time at which the isothermal period begins (T = 240 °C). The data shown are typical of thermal control samples indicating that the thermomechanical history of heat-pressed films leads to planar orientation of dipoles. This planar orientation may result from pellet alignment during film pressing which favors backbone orientation parallel to the thickness direction. Planar orientation of dipoles can also result from flow-induced planar stacking of molecular segments. As films are heated, the loss of this preferred backbone orientation would lead to a more random orientation of ester dipoles and this is consistent with experimental observation (f_{xy} approaches zero). It is interesting to note the long period of time involved in the gradual randomization.

Figure 6 shows results from an experiment in which an intermediate field (3150 V cm^{-1}) was applied during the

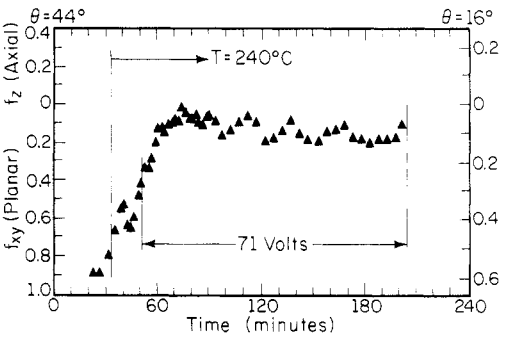

Figure 6. Fraction of oriented dipoles calculated with two different θ values as a function of time. Vertical lines indicate the onset of the isothermal period and application of the electric field (3150 V cm^{-1}).

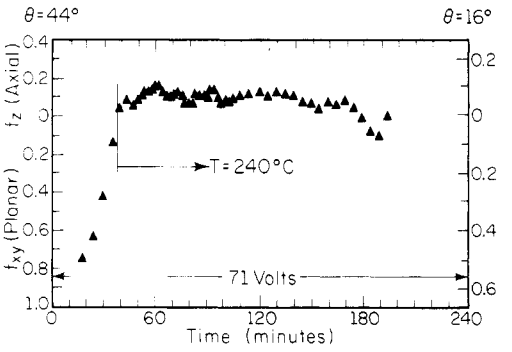

Figure 7. Fraction of oriented dipoles calculated with two different θ values as a function of time. The electric field (3150 V cm^{-1}) was applied at room temperature and maintained while heating and also during the isothermal period. A vertical line indicates the time when the isothermal period begins.

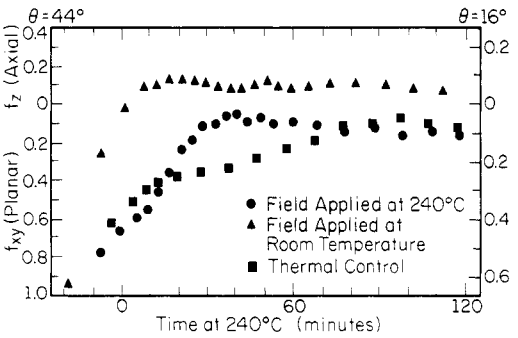

Figure 8. Fraction of oriented dipoles as a function of time (zero time corresponds to the onset of the isothermal period at 240 °C). The three curves correspond to a sample exposed only to the thermal program, a sample exposed to the electric field at 240 °C, and a sample exposed to the field at room temperature (3150 V cm^{-1}).

constant-temperature period (a vertical line in the figure indicates the time at which the electric field was applied). Since the ester dipole moment is almost orthogonal to the backbone axis, the observed reorientation is consistent with either dielectric alignment of dipolar groups (f_{xy} decreases) or randomization of backbone alignment. The difference between the thermal control and the field-exposed sample is a more rapid change to orientational states in which dipoles have greater components along the field direction. It is possible that an electrohydrodynamic instability contributes to the more rapid decrease of f_{xy}. Figure 7 shows data from an experiment in which the field was applied at room temperature prior to heating of the sample. A rapid and significant amount of axial realignment of dipoles is observed during the heating period. Twenty minutes into the constant-temperature period, the degree

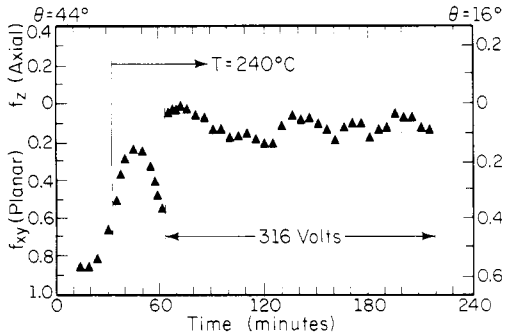

Figure 9. Fraction of oriented dipoles as a function of time in a sample exposed to a high electric field at 240 °C (14000 V cm^{-1}). The vertical lines indicate the onset of the isothermal period and the application of the field.

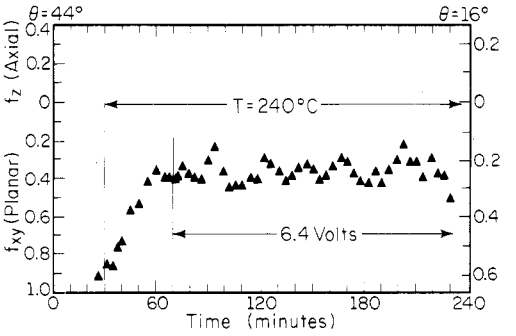

Figure 10. Fraction of oriented dipoles as a function of time in a sample exposed to a low electric field (285 V cm^{-1}). The vertical lines indicate the onset of the isothermal period and the application of the field.

of axial alignment reaches a maximum that is maintained for approximately 2 h. The significant effect of field application at room temperature is best appreciated in Figure 8 which plots dipolar orientation as a function of time for the thermal control and for samples exposed to the field after melting or at room temperature. The time axis in this figure was adjusted so that $t = 0$ corresponds to the time at which 240 °C was first reached in each experiment. In order to simplify Figure 8 and emphasize significant trends, values plotted were three-point moving averages of the experimental data. That is, three consecutive points were averaged and the value obtained was used to replace the second point of the sequence. The curves shown in Figures 5–7 contain the original data (without any averaging). Although all three samples tend toward axial or less planar dipolar alignment as a function of time, the electric field exposed samples do so at an increased rate. The sample exposed to the field at room temperature not only shows the most rapid realignment but also reaches a significantly higher degree of axial dipolar alignment. We do not know what determines the maximum value of orientation measured in these experiments. Kinetic factors related to the viscosity of the medium may limit the orientation that can be achieved during the time of observation.

It is clear that a significant extent of dipolar realignment cooperativity occurs in cases where the field is applied at room temperature. A possible implication of this fact is that interchain dipolar coupling facilitates cooperative dielectric alignment. The solid film should gradually pole upon heating when the field is applied at room temperature. If dipolar coupling occurs one might expect the formation of poled domains with large electric moments. As the melting range is approached (melting begins near 180 °C) some of these large moment domains may remain stable for a long time and align with the field. When the field is applied at high temperatures, dipolar coupling should be less prominent and domain sizes or their tendency to form would decrease. Dielectric alignment would then not be as cooperative as in the previous case.

Figure 9 shows the data obtained when a high electric field was used in the experiment (14000 V cm^{-1}). The maximum observed prior to field application might have been caused by flow in this particular sample. However, the important observation is that immediately upon application of the field, the trend toward planar orientation stopped and almost instantly changed to an orientation that could be interpreted as nearly random. The rapid change upon field application and the subsequent fluctuations in dichroic ratio could indicate the occurrence of an electrohydrodynamic instability involving turbulent flow. There are reports in the literature[13] of field-induced

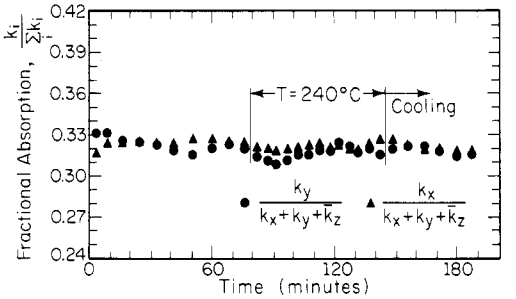

Figure 11. Time dependence of fractional carbonyl absorption in a thermal control corresponding to two orthogonal directions in the plane of the film.

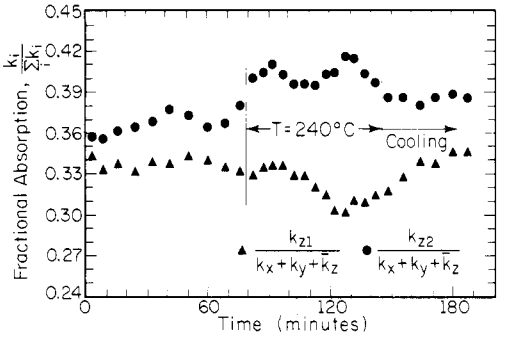

Figure 12. Time dependence of fractional carbonyl absorption along the thickness direction in a thermal control. The two curves correspond to the two different regions probed with the rotating cell ($\bar{k}_z = (k_{z1} + k_{z2})/2$).

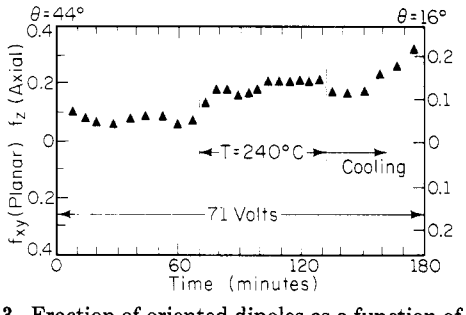

Figure 13. Fraction of oriented dipoles as a function of time for a sample exposed to an electric field of 3150 V cm^{-1}. The field was applied at room temprature and maintained, while heating, during the isothermal period in the liquid-crystalline state and also during solidification. The measurements were carried out with the rotating cell.

turbulence in LCP's when applied voltages are high. In contrast to the behavior observed at high fields, Figure 10 shows results from a low-field experiment (285 V cm^{-1}). Planar alignment diminishes at constant temperature but the rapid or gradual change observed upon application of

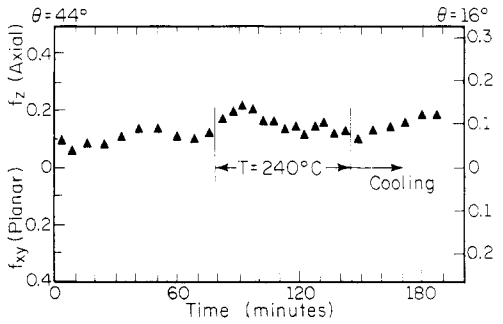

Figure 14. Fraction of oriented dipoles as a function of time for a thermal control sample. The measurements were carried out with the rotating cell.

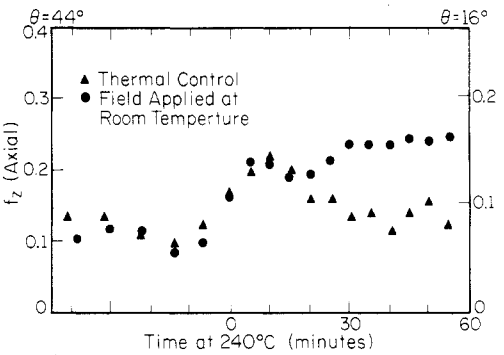

Figure 15. Comparison of axial alignment of dipoles in a thermal control sample and one exposed to the electric field while heating to an isothermal period at 240 °C. The measurements were carried out in the rotating cell.

high and intermediate fields, respectively, does not seem to occur in this case.

Results from experiments which used the rotating cell are shown in Figures 11–16. The data correspond to thermal controls or samples exposed to an intermediate electric field of 3150 V cm^{-1}. As mentioned before, when using the rotating cell, samples were premelted and solidified in contact with the crystals prior to spectroscopic analysis. An important observation is that all these samples had initial values of dichroic ratio which gave values of $f_z > 0$. This implies that after the first thermal cycle chains within the probed volume tend to acquire planar orientation with dipoles preferring directions that have finite projections on the normal to the silicon surface. Another important observation from rotating-cell experiments is that fractional absorption coefficients along the x and y directions are fairly similar (see Figure 11). This indicates that the assumption $k_x = k_y$ is reasonable when analyzing data from the standard cell. However, the two calculated values of fractional absorption coefficient along the z-direction obtained when using the rotating cell (see eq 3–6) differ more, suggesting backbone orientation differences along the thickness direction in the two volumes probed by the rotating cell (see Figure 12). The ratio of axial to planar absorbance used in calculating the dipolar orientation distribution was therefore based on an average of the values obtained in the two orientations of the cell,

$$\frac{k_z}{k_{x,y}} = \frac{k_{z1} + k_{z2}}{k_x + k_y} = \frac{2\bar{k}_z}{k_x + k_y} \tag{12}$$

Figure 13 shows results for a sample in the rotating cell exposed to the electric field at room temperature prior to melting. As can be seen in the dipolar orientation plot, an increase in axial dipolar alignment occurs upon melting. This higher level of axial alignment is maintained throughout the constant-temperature period, with a further increase noted upon solidification. The second vertical line

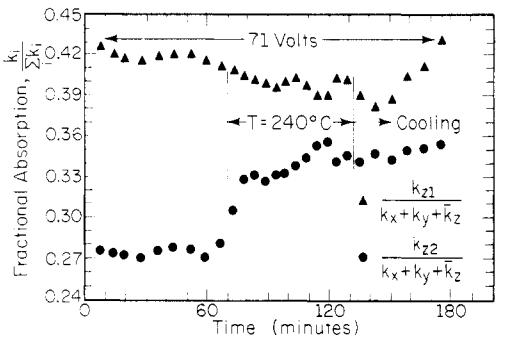

Figure 16. Time dependence of carbonyl fractional absorption along the thickness direction of the sample. The two curves correspond to the two different regions probed by the rotating cell.

in the figure indicates the onset of cooling under the influence of the field. Equivalent data for a thermal control is shown in Figure 14. The plot in Figure 15 shows clearly that while in the liquid crystalline state (at 240 °C) the sample under the influence of the field maintains a greater axial alignment of polar groups. This axial alignment can occur when the backbone axes prefer the plane of the film. A comparison of the data in Figures 13 and 14 after solidification (beyond the second vertical line) shows that polar alignment of dipoles under the field could very well lie in the range of 4–10%. It is very likely that the increase in f_z upon cooling under the field is associated with dipole rather than backbone reorientation. This is suggested on the basis that any alignment of the backbone in the liquid-crystalline state due to dielectric constant anisotropy would either be frozen or destroyed by solidification. Thus, the significant increase in f_z upon cooling is believed to be the result of dipolar reorientation along the thickness direction of the solidifying film. The question of dipolar orientation in the field is of great interest since a calculation using a Lorentz internal field predicts that 0.3% of the dipoles should align in the field. The observed difference amounting to 1 order of magnitude or more must be caused by significant levels of dipolar coupling in these main-chain liquid-crystal polymers.

An important point revealed in data obtained with the rotating cell is how the response of the material to the applied field depends on the initial dipolar orientation. This can be seen most clearly in Figure 16 which shows changes in fractional absorption coefficient along the field direction in two different locations of the same sample. The smaller of the two values increases rapidly upon melting whereas the larger one does not seem affected as much by field application and decreases presumably because of other acting forces. The significant dielectric misalignment of dipoles in one of the locations creates a strong electric torque which drives the reorientation. It is also interesting to note that upon cooling, the location with greater planar orientation of "chains" ($f_z > 0$) acquires greater axial orientation of dipoles along the field direction. This can be understood on the basis that dipoles lying in planes normal to the backbone axis rotate easily toward the field direction as the fluid phase solidifies.

Conclusions

Infrared spectroscopic experiments during application of an electric field to a main-chain liquid-crystal polymer have revealed several fundamental properties of these polymers. These chains seem to rapidly acquire and maintain dielectric alignment of dipoles when poling occurs before or during the solid-to-liquid crystal transformation. When the liquid crystal is solidified under the field the

extent of polar alignment for moments nearly orthogonal to the backbone could lie in the range 4–10%. This range suggests that interchain dipolar coupling is an important phenomenon in these polymers. On this basis one may expect that localized ferroelectric ordering enhances cooperative behavior during the transition from poled solid to liquid crystal. The observed phenomena could be useful in the formation of polymeric solids with electrical or nonlinear optical properties.

Acknowledgment. This work was supported through a research grant from the 3M Co.

Appendix

$$\alpha = 4n_2^2/[n_1^2(\tan\theta)(1 - n_2^2/n_1^2 \sin^2\theta)^{1/2}(1 - n_2^2/n_1^2)]$$

$$\beta = [4n_2^2(1 - n_2^2/n_2^2 \sin^2\theta)]/[n_1^2(\tan\theta)(1 - n_2^2/n_1^2 \sin^2\theta)^{1/2}(1 - n_2^2/n_1^2 \sin^2\theta + n_2^4 \cot^2\theta/n_1^4)]$$

$$\gamma = 4n_2^2/[n_1^2(\tan\theta)(1 - n_2^2/n_1^2 \sin^2\theta)^{1/2}(1 - n_2^2/n_1^2 \sin^2\theta + n_2^4 \cot^2\theta/n_1^4)]$$

Registry No. (*p*-Acetoxybenzoic acid)(ethylene glycol)(terephthalic acid) (terpolymer), 52237-98-6.

References and Notes

(1) Carr, E. F. *Mol. Cryst. Liq. Cryst.* **1969**, *7*, 253.
(2) Wise, R. A.; Olah, A.; Doane, J. W. *J. Phys.* **1975**, *36*, 117.
(3) Moore, J. S.; Stupp, S. I. *Macromolecules* **1987**, *20*, No. 2.
(4) Martin, P. G.; Stupp, S. I. *Polymer* **1987**, *28*, 897.
(5) Martin, P. G.; Moore, J. S.; Stupp, S. I. *Macromolecules* **1986**, *19*, 2459.
(6) Landreth, B. M.; Stupp, S. I. *J. Appl. Spectrosc.* **1986**, *40* (7), 1032.
(7) Jackson, W. J.; Kuhfuss, H. F. *J. Polym. Sci.* **1976**, *14*, 2043.
(8) Flourney, P. A.; Schaffers, W. J. *Spectrochim. Acta* **1966**, *22*, 5.
(9) Economy, J.; Storm, R. S.; Matkovich, V. I.; Cottis, S. G.; Nowak, B. E. *J. Polym. Sci., Polym. Chem. Ed.* **1976**, *14*, 2207.
(10) Flory, P. J. *Statistical Mechanics of Chain Molecules*; Wiley: New York, 1969; p 184.
(11) Liang, C. Y.; Krimm, S. *J. Mol. Spectrosc.* **1959**, *3*, 554.
(12) Bradbury, E. M.; Elliot, A.; Fraser, R. D. B. *Trans. Faraday Soc.* **1960**, *56*, 1117.
(13) Gilli, J. M.; Bosch, A. T.; Pinton, J. F.; Sixou, P.; Thomas, O.; Blumstein, A.; Blumstein, R. B. *Mol. Cryst. Liq. Cryst.* **1984**, *105*, 375.

Spectroscopic Analysis of Phase Separation Behavior of Model Polyurethanes

Han Sup Lee, Ying Kang Wang,† and Shaw Ling Hsu*

Polymer Science and Engineering Department, The University of Massachusetts, Amherst, Massachusetts 01003. *Received February 17, 1987*

ABSTRACT: Infrared spectra as a function of temperature have been obtained for model polyurethanes. Unique spectroscopic features in the N—H and C=O stretching regions have been found for rapidly cooled samples. The changes of these newly found features have been useful in the interpretation of the phase-separation behavior. A direct correlation between changing hydrogen bonding characteristics in soft and hard domains and macroscopic phase transformation as a function of temperature has been presented.

Introduction

Segmented polyurethanes are copolymers that consist of hard and soft segment units. Due to incompatibility between the two types of structural units, it is generally agreed that the polymers formed undergo microphase separation resulting in hard-segment-rich hard domains, soft-segment-rich soft matrix, and poorly characterized interphase. Since the glass-transition temperatures (T_g) of soft segments and hard segments are well below and higher than the usual service temperature, i.e., usually room temperature, respectively, polyurethanes are thermoplastic elastomers with a wide range of mechanical properties depending on the ratio of the two structural components.

Even though the phase-separated domain structure is not unique to polyurethane, it is geneally accepted that the strength and high elasticity of polyurethanes are due to the hard domains stabilized by the hydrogen bonding between hard segments.[1] The perfection and degree of phase separation have been found to be important to the properties of polymers and are dependent on molar composition, synthesis procedure, and thermal history.[2,3] Hydrogen bonding may form between the N—H and C=O groups in the hard domain. If polyether is part of the polymer, then hydrogen bonding between the N—H group of hard segment dispersed in the soft matrix and the C—O—C group of soft segment has also been suggested.[4-7] Because of its importance, hydrogen bonding properties of urethane functional groups have been extensively investigated. Spectroscopic techniques, mainly infrared, have complemented other characterization techniques to better understand the phase-separated structures of polyurethanes. Even though a considerable amount of information has been obtained, a direct interpretation of the spectroscopic data is still difficult. More recently, these difficulties have again been mentioned in the literature.[8-11]

It is well-known that polyurethane structures and properties change as a function of temperature and these changes have been followed by thermal analysis,[12-14] spectroscopy,[8,9,14-16] dynamic mechanical analysis,[1,18,19] wide-angle X-ray diffraction,[20,21] and small-angle X-ray scattering.[22] Several processes have been suggested to occur concurrently as a function of temperature. These structural changes are (1) weakening and disassociation of H bonding; (2) disordering of hard segment domain; (3) hard–soft segment mixing; and (4) thermal degradation, mainly occurring in urethane linkages.[23] Vibrational spectroscopy, more specifically, infrared technique, has demonstrated its particular usefulness in characterizing the hydrogen bonding characteristics in each domain. Some of the localized vibrations such as the N—H stretching vibration or C=O stretching vibration are strongly perturbed by the formation of hydrogen bonds. Both the frequency shifts and intensity changes are

* To whom correspondence should be addressed.
† Present address: Department of Chemistry, Peking University, Beijing, People's Republic of China.

0024-9297/87/2220-2089$01.50/0